Analysis and Design of Missile and Aircraft Control Systems

K. W. HAN*
Chinese Naval College of Technology, Taiwan

AND

G. J. THALER†
Naval Postgraduate School, Monterey, Calif.

The root locus method is extended to multiparameter problems by partitioning the characteristic equation into terms with even powers of s, and terms with odd powers of s, then rearranging in root locus form. For the indicated partition, the poles and zeros all are on the imaginary axis (normally), stability depends on the sequence in which they occur, and dynamic performance is related to the spacing between poles and zeros. By treating the numerator and denominator polynomials separately, response can be studied as a function of two adjustments. This technique can be used when there are more than two adjustable parameters. For most problems, these manipulations become cumbersome in the same fashion that conventional stability analysis techniques are cumbersome for more than one parameter. In addition, the time required for solution is reduced severalfold. Used in conjunction with describing functions, the stability curves provide a means of analyzing nonlinear systems and predicting limit cycles. Application to the identification problem in adaptive systems seems possible.

Nomenclature

$s = \sigma + j\omega$	=	complex variable
$F(s)$	=	characteristic polynomial in s
$F_e(s), F_o(s)$	=	polynomials consisting of the even- and odd-powered terms from the characteristic polynomial
$z_1, z_2, \ldots$	=	roots of $F_e(s)$
$p_0, p_1, \ldots$	=	roots of $F_o(s)$
y	=	s^2
θ	=	pitch angle
$S_{rg} = K_2$	=	sensitivity (gain) of rate gyro
$S_{\mathrm{amp}} = K_1$	=	sensitivity (gain) of main amplifier
η	=	$4.25K_1$
$S_{ig} = K_3$	=	sensitivity (gain) of integrating gyro
N_1	=	describing function of ideal relay
δ_e	=	elevator deflection angle
$\dot{\theta}$	=	pitch rate

Introduction

In the preliminary stages of analysis and design for dynamic systems, frequency response methods (Bode-Nichols)[1] or conventional root locus methods usually are applied, followed (where needed) by computer studies. Frequency response methods can be inconvenient when studying the effects of minor feedback loops (which are common in aircraft and missile problems) while both frequency response and root locus methods are largely restricted to problems involving one variable parameter.

The methods proposed in this paper are based on a relatively simple variation of the root locus technique. It is observed that the characteristic equation may be partitioned into a sum of two polynomials:

$$F(s) = F_e(s) + F_o(s) = 0 \tag{1}$$

where $F_e(s)$ is the sum of all terms containing even powers of s, and $F_o(s)$ is the sum of all terms containing odd powers of s. Equation (1) can be put in standard root locus form:

$$F_e(s)/F_o(s) = -1 \tag{2}$$

Received August 19, 1966; revision received December 5, 1966. [7.03, 7.05]

* Associate Professor, Department of Electrical Engineering; also Adjunct Associate Professor, National Chiao Tung University, Hsinchu, Taiwan.

† Professor of Electrical Engineering. Associate Fellow AIAA.

Equation (2) may be used to construct root loci if desired, and this is often helpful. A slightly different viewpoint provides a convenient stability criterion; stability curves; and the means to analyze the effects of several parameters, nonlinearities, and other features that are indicated in the following paragraphs.

A Stability Criterion[5] and Methods of Predicting Characteristic Roots

If the characteristic equation is partitioned and rearranged as in Eqs. (1) and (2), it is readily shown[5] that all zeros and poles of Eq. (2) must lie on the imaginary axis of the s plane and their absolute values must be related as

$$p_0 < z_1 < p_1 < z_2 < p_2 \ldots \tag{3}$$

if the characteristic equation is to have all roots in the left half plane so that the system will be stable.

The polynomials $F_e(s)$ and $F_o(s)$ must be factored, but each contains only alternate powers of s; thus a definition of variable $y = s^2$ reduces the order of these polynomials by a factor of 2, making stability analysis of a fifth-order equation very simple, and analysis of a seventh-order equation only slightly more difficult since thd cubics formed are required to have all real roots in order to satisfy the stability criterion of Eq. (3). Analysis of equations of order greater than seventh unavoidably involves some labor. It should be noted that the partitioning process provides two polynomials that are treated separately in establishing the stability relations of Eq. (3), and it is apparent that one variable parameter can always be permitted in *each* polynomial. Thus stability analysis in terms of two parameters usually will be available, and for some problems additional parameters may be permissible.

From Eq. (3), it is seen that the stability limit is reached when a pole is exactly equal to a zero. When the system is stable, all roots are known to be in the left half plane, and it can also be shown[5] that all *root loci* are entirely in the left half plane except for the terminating poles and zeros on the imaginary axis. For specific cases, the root loci may be drawn accurately if desired, but often a sketch permits rapid estimate of dynamic response. Note that the root locus segments, since they begin on poles and end on zeros, usually have the shape of a "lobe" (see Figs. 1 and 2), for which a rough approximation is a semicircle with diameter equal to the

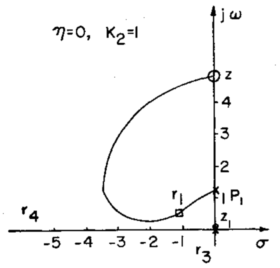

Fig. 1 Root loci of a displacement autopilot.

spacing between pole and zero. Then the *maximum* value of the real part of the complex root is approximately half of the spacing between pole and zero. This permits a quick estimate of the *minimum* settling time of the mode of oscillation. In like manner, the root locus gains of the polynomial ratio of Eq. (2) can be used to estimate whether the roots are close to the poles or close to the zeros; and if this is done, a better value is obtained for settling time ζ, ω_n, etc. for each mode. These sketching rules tend to give pessimistic results, since the true shape of the lobes differs from the semicircular approximation (see Fig. 1) in such a way that the performance available from the system is usually better than that predicted by the approximations. More accurate values require quantitative calculations.

Stability Curves

The polynomials $F_e(s)$ and $F_o(s)$ define the zeros and poles of Eq. (3). Each of these polynomials may contain a variable parameter, and the stability curves simply are plots of the values of the zeros and poles as functions of the variable parameter. Inspection of the curves then defines the range of parameter values required for stability, etc. Since it is convenient to reduce the order of $F_e(s)$ and $F_o(s)$ by substituting $y = s^2$, it also is convenient to plot y vs the parameter value as a stability curve rather than the actual pole or zero value.

As an illustration, consider the autopilot of Fig. 3. The amplifier gain $S_{\text{amp}} \triangleq K_1$ is adjustable as is $S_{rg} \triangleq K_2$, the sensitivity of the rate gyro. The characteristic equation of this system is

$$s^4 + 10.805s^3 + (9.375 + 13.9K_2)s^2 + (13.25 + 4.25K_2 + 13.9K_1)s + 4.25K_1 = 0 \quad (4)$$

Let $y = s^2$ and $\eta = 4.25K_1$. Then the stability equations are

$$F_e(y) = y^2 + (9.375 + 13.9K_2)y + \eta = 0 \quad (5)$$

$$F_o(y) = y + 0.393K_2 + 1.2221 + 0.302\eta = 0 \quad (6)$$

$$y = 0$$

The equation $y = 0$ indicating a pole at the origin obtains from the fact that the polynomial consisting of odd-powered

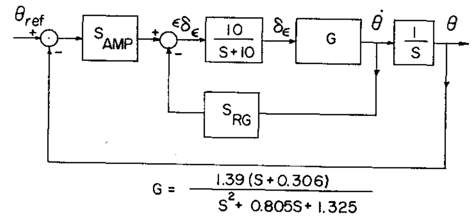

Fig. 3 Block diagram of a displacement autopilot of a jet transport.

terms always provides a root at $s = 0$. Both stability equations are functions of two parameters K_2 and η, so a family of stability curves results. Sample curves are shown on Fig. 4 for $K_2 = 0, 1, 2$. A vertical line drawn at any chosen value of η intersects both stability curves (for a chosen K_2). The sequence of these intersections defines the sequence of pole-zero locations on the imaginary axis of the s plane. The stability limit (for a chosen value of K_2) is at the intersection of the two stability curves. Thus for $K_2 = 1$ the two curves intersect at $\eta = 60°$, indicating that $p = z = r$ so that pure imaginary roots exist for $K = 1$, $\eta = 60$.

Assuming $\eta = 0$ and $K_2 = 1$, the pole-zero locations are determined from Fig. 4 (and the equation $y = 0$) and are plotted on the s plane of Fig. 1. The condition $y = 0$ provides a pole at the origin, and the z_1^2 curve [see Eq. (8)] passes through the origin for $\eta = 0$ so z_1 is a double zero at the origin. This provides a closed root locus with r_3 also at the origin. Root locus also extends from the second zero at the origin along the negative real axis and provides a real root r_4 far out on the negative real axis (because the root locus gain is low for the function F_e/F_o). The p_1^2 curve gives poles at $j\omega \cong \mp 1.25$, and the z_1^2 curve gives zeros at $j\omega \cong \mp 4.8$. The root locus lobe is shown on Fig. 1 (computer-calculated rather than sketched) and the root r_1 is close to the pole p_1 because the root locus gain is low. Note that the root locus is drawn for a function that has a fixed gain; i.e., there is no parameter that moves the roots *along* this locus; rather, the two variable parameters η and K_2 can be used to relocate the poles and zeros and thus control the stability, reshape the locus, and relocate the roots. The only purpose of sketching the root locus on the s plane is to aid in the visualization of the root locations and to help analyze the effects of changes in η and K_2. The actual root locations have been estimated in Fig. 1. If more accurate results are desired, the magnitude rule can be applied in the usual way.

A second illustration is the pitch control system for a longitudinal autopilot shown in Fig. 5. Here one problem is to find, if possible, a setting for the gyro gains such that the system is stable and has acceptable dynamic response for both high and low angles of attack.

From Fig. 5 the characteristic equation and the stability equations may be obtained for both conditions of operation. At low angle of attack the characteristic equation is

$$s^4 + 10.9s^3 + (17 + 150K_2)s^2 + (80 + 60K_2 + 150K_1)s + 60K_1 = 0 \quad (7)$$

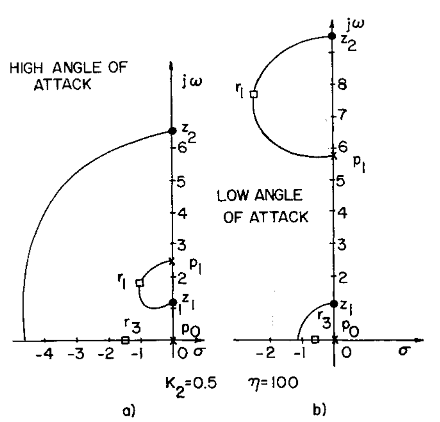

Fig. 2 Root loci of a control system for longitudinal autopilot.

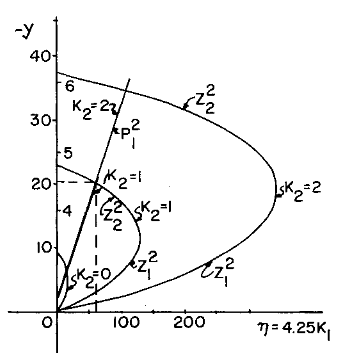

Fig. 4 Stability curves of a displacement autopilot.

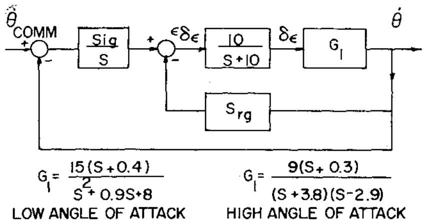

Fig. 5 Block diagram of a pitch orientational control system for longitudinal autopilot.

Letting $y = s^2$ and $60K_1 = \eta$, the stability equations are:

$$F_e(y) = y^2 + (17 + 150K_2)y + \eta = 0 \quad (8)$$

$$F_o(y) = y + 7.35 + 6.5K_2 + 0.23\eta = 0 \quad (9)$$

$$y = 0$$

At high angle of attack the characteristic equation is:

$$s^4 + 10.9s^3 + (90K_2 - 2)s^2 + (27K_2 + 90K_1 - 110)s + 27K_1 = 0 \quad (10)$$

and the stability equations become:

$$F_e(y) = y^2 + (90K_2 - 2)y + 0.45\eta = 0 \quad (11)$$

$$F_o(y) = y + 2.475K_2 - 10.1 + 0.138\eta = 0 \quad (12)$$

$$y = 0$$

Both pairs of stability equations are plotted in Fig. 6 for $K_2 = 0.5$, providing a graphical arrangement that permits analysis of the compatability of low-angle and high-angle performance as a function of η with K_2 fixed. For complete study, a range of K_2 values must be used.

From Fig. 6 it is observed that the low angle-of-attack system has a stability limit at $\eta = 320$, whereas the high angle-of-attack system has a stability limit at $\eta = 60$. Thus the range of possible values for η clearly is defined as $60 < \eta < 320$. Inspection of the curves indicates that the upper limit of η can be increased by increasing K_2, but the lower limit will not be changed appreciably by K_2 adjustments.

Since operation of the system must be between the stability limits, this range of η values is investigated to find the most suitable adjustment. Figure 2 shows the root locus plot for $K_2 = 0.5$ and $\eta = 100$, with approximate locations for the roots. It is estimated that the real root r_3 dominates the low angle-of-attack performance, whereas the complex roots r_1 will be important in the high angle-of-attack performance, but with significant contribution from the real root r_3. If the value of η is increased, z_1 and p_1 both move to larger values for both angles of attack with the result that r_1 becomes less important in the high angle-of-attack case, and the response of the low angle case becomes a bit faster. A "best" value of η can thus be arrived at, for K_2 set at 0.5. Of course the study should be repeated for a range of values for K_2. Such results provide adequate guidance for more detailed computations or for simulation studies.

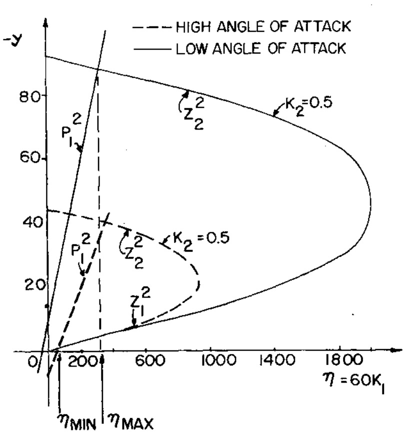

Fig. 6 Stability curves of a control system for longitudinal autopilot.

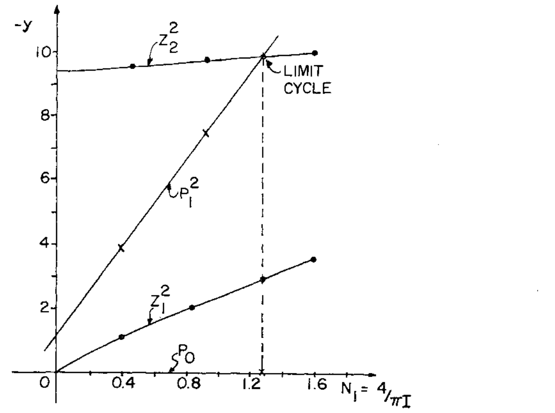

Fig. 7 Stability curves of a nonlinear system.

These methods can be extended to some problems with more than two adjustable parameters. However, the technique is somewhat cumbersome when applicable; thus no illustration is given here.

Nonlinear Systems

The stability curve technique can be extended to the analysis of nonlinear systems, it can predict limit cycles, and may provide information of value for adaptive control schemes. Since root locus methods are derived from linear equations, the nonlinear model of the system must be linearized before the stability curve method can be used. It is assumed that this linearization is accomplished by using describing functions to represent the nonlinearities, and it is implicit in this assumption that the nonlinear loops involved have frequency response characteristics that justify the use of describing functions. The stability equations are formulated, and the variable parameter is chosen to be the describing function of the nonlinearity. Thus the pole-zero locations vary as a function of the amplitude of the driving signal, and limit cycles are defined at the intersections of the stability curves.

As an illustration, consider the system of Fig. 3 with an added nonlinear element that is to be an ideal relay with unity saturation level located in cascade with the input to G. Use N_1 as symbol for the describing function of the ideal relay. For this illustration let

$$G = 0.139(s + 30)/(s^2 + 0.8s + 1.33) \quad (13)$$

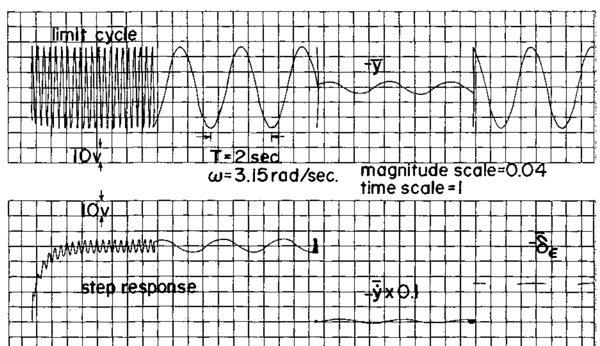

Fig. 8 Analog computer results for a nonlinear system.

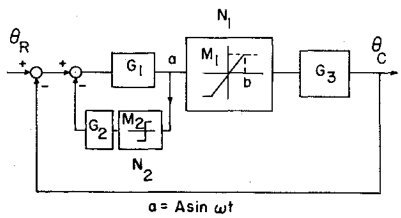

Fig. 9 Control system with two nonlinear elements.

Then the characteristic equation becomes

$$s^4 + 10.8s^3 + (9.33 + 1.39N_1K_2)s^2 + (13.3 + 41.7K_2N_1 + 1.39K_1N_1)s + 41.7K_1N_1 = 0 \quad (14)$$

The stability equations are:

$$F_e(y) = y^2 + (9.33 + 1.39K_2N_1)y + 41.7K_1N_1 = 0 \quad (15)$$

$$F_o(y) = y + 1.23 + 3.86K_2N_1 + 128K_1N_1 = 0 \quad (16)$$

$$y = 0$$

For chosen K_1 and K_2, both relationships are functions of N_1 only, and stability curves can be plotted on a y vs N_1 plane. For $K_1 = 0.563$ and $K_2 = 2$ the results are given in Fig. 7, which predicts a limit cycle at the intersection of the two stability curves. For the indicated value of N_1, the limit cycle has $\omega = 3.15$ and from describing function theory its amplitude should be $I = 0.99$. Analog computer verification is given in Fig. 8.

Some additional analyses are possible. Under conditions of limit cycle operation, $s = 0 + j\omega$ and the stability equations become

$$\omega^4 - (9.33 + 1.39K_2N_1)\omega^2 + 41.7K_1N_1 = 0 \quad (17)$$

$$-\omega^2 + 1.23 + 3.86K_2N_1 + 0.128K_1N_1 = 0 \quad (18)$$

Choice of ω and N reduce 17 and 18 to linear equations in K_1 and K_2, so loci of constant ω and/or constant amplitude I for the limit cycle can be plotted on a K_1 vs K_2 plane. From such a plot the limit cycle can be designed by choice of K_1 and K_2, and the sensitivity of the limit cycle characteristics to changes in K_1 and K_2 may be determined. If the system is suitable for a self-adaptive scheme in which K_1 and K_2 represent variable parameters, the changes in frequency and amplitude of the limit cycle can be used for identification purposes.

The basic technique can also be extended to systems with several nonlinear elements. A simple example is given in Fig. 9, where both nonlinearities are fed with the same signal. Let $G_1 = 10/(s + 1)$; $G_2 = s + 10$; $G_3 = 10/(s + 1)^2$; $b = 1$; $M_1 = 1000$; $M_2 = 10$; N_1 and N_2 are describing functions. Then the characteristic equation is

$$s^3 + \frac{120N_2 + 3}{10N_2 + 1}s^2 + \frac{210N_2 + 3}{10N_2 + 1}s + \frac{100(N_1 + N_2) + 1}{10N_2 + 1} = 0 \quad (19)$$

and the stability equations are

$$F_e(y) = y + \{[100(N_1 + N_2) + 1]/(120N_2 + 3)\} = 0 \quad (20)$$

$$F_o(y) = y + [210N_2 + 3/(10N_2 + 1)] = 0 \quad (21)$$

Both N_1 and N_2 are explicit functions of the signal amplitude

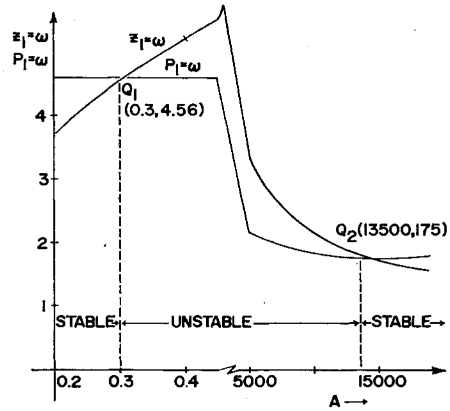

Fig. 10 Stability curves for system of Fig. 9.

A at point a:

$$N_1 = \frac{M_1}{\pi}\left[2\sin^{-1} b/A - \frac{2b}{A^2}(A^2 - b^2)^{1/2}\right] + \frac{4M_1}{\pi A_2}(A^2 - b^2)^{1/2} \quad (22)$$

$$N_2 = \frac{4M_2}{\pi A} \quad (23)$$

Thus Eqs. (20) and (21) may be plotted vs the common parameter A; and the intersections, as shown in Fig. 10, predict the existence, amplitude, and frequency of the limit cycles. These results also have been verified with the analog computer.

Conclusion

The root locus method has been extended to two parameter problems by partitioning the characteristic equation in even- and odd-powered polynomials that are then manipulated into root locus form. A "stability curve" method has been presented which simplifies system analysis and permits logical choice of numerical values for the adjustable parameters. Thus ready solution is obtained for problems that are cumbersome by conventional methods, and the time required for solution is reduced severalfold. It also has been shown that the method can be applied to some nonlinear systems to predict the existence, frequency, and amplitude of limit cycles.

References

[1] Horowitz, I. M., *Synthesis of Feedback Systems* (Academic Press Inc., New York, 1963).

[2] Blakelock, J. H., *Automatic Control of Aircraft and Missiles* (John Wiley & Sons Inc., New York, 1965).

[3] Siljak, D. D., "Analysis and synthesis of feedback control systems in the parameter plane, Part I. Linear control systems," IEEE, Trans. Appl. Ind. **83,** 449–458 (November 1964).

[4] Han, K. W. and Thaler, G. J., "Analysis and design of control systems using parameter space method," IEEE, Trans. Autom. Control **AC-11,** 560–563 (July 1966).

[5] Han, K. W. and Thaler, G. J., "High order system analysis and design using root locus method," J. Franklin Inst. **281,** 99–113 (February 1966).

[6] Liu, S. H. and Thaler, G. J., "An analytical method for analysis and design of control systems," IEEE, Trans. Autom. Control **AC-10,** 49–59 (January 1965).